The Journal of Experimental Biology 199, 2667–2677 (1996)
Printed in Great Britain © The Company of Biologists Limited 1996
JEB0464

ANALYSIS OF CARDIAC SHUNTING IN THE TURTLE *TRACHEMYS* (*PSEUDEMYS*) *SCRIPTA*: APPLICATION OF THE THREE OUTFLOW VESSEL MODEL

ATSUSHI ISHIMATSU*, JAMES W. HICKS† AND NORBERT HEISLER‡,§
Max-Planck-Institut für experimentelle Medizin, Hermann-Rein-Straße 3, D-37075 Göttingen, Germany

Accepted 15 July 1996

Summary

Blood distribution within the ventricle was analysed in acutely prepared turtles *Trachemys scripta* by measuring the oxygen concentration and flow rates of blood in the central vessels. Pulmonary ($\dot{Q}_p$) and systemic ($\dot{Q}_s$) blood flow rates were similar when total cardiac output ($\dot{Q}_{tot}$) was below 40 ml min^{-1} kg^{-1}. Above this value, increments of $\dot{Q}_{tot}$ were directed to the pulmonary circuit, with $\dot{Q}_s$ levelling off at approximately 20 ml min^{-1} kg^{-1}. When $\dot{Q}_{tot}$ was larger than 40 ml min^{-1} kg^{-1}, the systemic circuit was almost exclusively perfused by left atrial blood and systemic venous return was almost all directed towards the lungs. Blood oxygen levels and flow rates were consistently higher in the right aorta than in the left aorta. Blood movement within the ventricle, coupled with differences in ejection timing, is probably the decisive factor determining this pattern of blood distribution in the turtle heart.

Key words: turtle, cardiac shunting, blood partitioning, three outflow vessel model, *Trachemys scripta*.

Introduction

The anatomically undivided ventricle of noncrocodilian reptiles has two inflow openings and three outflow vessels. The ventricular lumen of these animals is also divided into two subcavities. Two atria open into the dorsally located cavum dorsale (CD), which is often further subdivided into the cavum venosum (CV) on the right and the cavum arteriosum (CA) on the left, although such differentiation has not always been described (see Van Mierop and Kutsche, 1985). The right and left aortae (RAo and LAo respectively) arise from the right side of the CD. The cavum pulmonale (CP) is a smaller chamber located ventrally and to the right of the CD. The CP has no direct communication with either of the atrial orifices and is incompletely separated from the CD by a horizontal muscular septum. The pulmonary artery (PA) emerges from the CP. This complex spatial arrangement indicates that blood may be translocated within the ventricle during each cardiac cycle, resulting in intracardiac shunting. However, little information is available regarding details of blood movement within reptilian ventricles.

Cardiac shunting has been conventionally defined as either right-to-left (R–L) or left-to-right (L–R). A R–L shunt represents a fraction of the systemic venous blood being recirculated into the systemic circulation. A L–R shunt represents a fraction of the pulmonary venous blood flowing back into the pulmonary circulation. The conventional analysis of cardiac shunting in reptiles assumes identical blood oxygen levels in the two aortae (e.g. Burggren and Shelton, 1979). Therefore, four blood pathways, shunted and unshunted flows from each atrium into the pulmonary and systemic circuits, were assumed to exist. However, several studies have reported that oxygen levels in the two aortae are different (Khalil and Zaki, 1964; Tucker, 1966; Baker and White, 1970; Burggren and Shelton, 1979; Ishimatsu *et al.* 1988). This fact led us to develop a model delineating the six possible blood flow pathways within the ventricle (the three outflow vessel model, Ishimatsu *et al.* 1988).

The three outflow vessel model can be tested using several approaches. Our previous study on the Nile monitor lizard *Varanus niloticus* was performed by combining blood gas analysis and the microsphere method for determination of relative flow rates (Ishimatsu *et al.* 1988). Although cardiac shunting patterns could be demonstrated for chronically cannulated, recovered animals, this approach did not allow the analysis of blood flow distribution in terms of absolute flow rates. In the present study, this gap has been filled by measuring flow rates and oxygen levels of blood in all central vascular

*Present address: Nomo Fisheries Station, Nagasaki University Nomozaki, Nagasaki 851-05, Japan.
†Present address: Department of Ecology and Evolutionary Biology, University of California at Irvine, Irvine, CA 92717, USA.
‡Present address: Department of Animal Physiology, Humboldt Universität zu Berlin, D-10115 Berlin, Germany.
§Author for correspondence at the following address: Tierphysiologie, Math. Nat. Fak. I, Humboldt Universität zu Berlin, Abderhaldenhaus, Philippstraße 13, D-10115 Berlin, Germany (e-mail: heisler@biologie.hu-berlin.de).
This paper is dedicated to the memory of Mrs Sylvia Glage, who made our life in Göttingen most enjoyable and productive.

sites in an acute preparation of a turtle, *Trachemys* (*Pseudemys*) *scripta*. To extend this study to cover the dynamic range of blood flow rates, stimulation of the cervical vagus was used as a tool for an extended analysis of shunting patterns.

Materials and methods

Animals

Turtles, *Trachemys* (*Pseudemys*) *scripta* Gray, were purchased from a commercial animal dealer (Lemberger, Oshkosh, WI, USA) and airfreighted to Germany. They were kept in large aquaria with dry basking areas and infrared lamps to allow behavioural regulation of body temperature. Water temperature in the aquaria was set at 25±1 °C. Animals were regularly fed chopped beef liver and chicken meat. Food was withheld for 3 days before experimentation.

Surgery

Anaesthesia was induced as described by Hicks and Malvin (1992). Animals were then tracheotomized and mechanically ventilated (12–20 min^{-1}) with a humidified gas mixture of 17 % O_2, 3 % CO_2 and 80 % N_2 prepared using a gas-mixing pump (Wösthoff, Bochum, Germany). A rectangular opening (approximately 3 cm×4 cm) was cut in the plastron with a bone saw to expose the heart and central blood vessels. The plastron piece was carefully removed from the underlying musculature. Bleeding from the musculature was stopped by cauterization. Short sections of the central vessels were freed from surrounding connective tissues and blood flow probes (2R ultrasound, transit-time blood flow probes; Transonic Systems Inc., Ithaca, NY, USA) were placed around the left pulmonary artery (PA), the LAo, the common carotid of one side (CC) and the main trunk of the right aorta (RAo,t). Care was taken not to kink or distort the vessels. Subsequently, five central vascular sites [PA, LAo, RAo,t, the left atrium (LAt) and the right atrium (RAt)] were non-occlusively catheterized as described by White *et al.* (1989). A thin thermistor was inserted into the cloaca to measure body temperature.

The cervical vagus on each side was exposed and prepared for nerve stimulation as described by Hicks and Comeau (1994). A few animals showing vasoconstriction following probe or catheter placement were excluded from data analysis.

Protocol

During experimentation, animals were placed supine and mechanically ventilated as described above. Experiments were performed on seven turtles at 25±1 °C.

The first set of measurements was conducted to obtain blood gas levels and flows with intact vagi (V_{intact}). Blood samples were drawn simultaneously from the five sites while blood flows were recorded continuously. Immediately after withdrawal, blood was analyzed for P_{O_2}, P_{CO_2} and pH and was subsequently reinfused into the animal to minimize blood loss.

After completing the first set of measurements, the vagi were exposed and sectioned as described above. Five different conditions for vagal stimulation were tested. These included measurements without electrical stimulation (V_{cut}), efferent stimulation of either right (RVEF) or left (LVEF) vagus, and afferent stimulation of either right or left vagus (RVAF and LVAF, respectively). Electrical conditions of stimulation were as follows: 1–3 Hz, 4–8 V and 200 ms. Animals were allowed to stabilize between stimulation periods. In three animals, sodium nitroprusside (32 μg) was injected as a bolus into the right atrium (RAt) to evoke extreme deviations of cardiovascular conditions. Nitroprusside injection tended to give lower α (see below) values, while no apparent effects were seen in the other partition fractions.

Analytical methods

Blood P_{O_2}, P_{CO_2} and pH were determined using two sets of blood gas analyzers (Radiometer BMS3 Mk2) thermostatted to 25±0.1 °C. We used previously reported data on the oxygen dissociation curve for *T. scripta* (Burggren *et al.* 1977; Maginniss *et al.* 1980) to calculate oxygen content (C_{O_2}) from P_{O_2} and pH. Oxygen capacity was estimated from its relationship with haematocrit (Hct, %): O_2 capacity = 0.788+0.284Hct (J. W. Hicks, unpublished observation). Plasma bicarbonate concentration was calculated from pH and P_{CO_2} using values for pK'_1 (the apparent first dissociation constant of the bicarbonate buffer system in plasma) and CO_2 solubility reported by Nicol *et al.* (1983) for *Chrysemys picta bellii*. Two dual-channel Transonic flowmeters (T206, Transonic Systems Inc.) were used to determine blood flow in the four central blood vessels. Between blood sampling, catheters were connected to pressure transducers (Statham P23B) to record blood pressure.

Calculation of shunt

Flow partitioning of the blood derived from both atria into the PA, LAo and RAo was calculated by substituting C_{O_2} and blood flow data into equations previously reported (see equations 19–21 in Ishimatsu *et al.* 1988). Fractions of the inflow from the left atrium (LAt) into the ventricle are designated as α (to the PA), β (to the RAo) and 1–α–β (to the LAo). Fractions of the RAt inflow are referred to as *X* (to the LAo), *Y* (to the RAo) and 1–*X*–*Y* (to the PA).

To check the accuracy of the calculation, we compared the right aortic blood flow ($\dot{Q}_{RAo}$) derived from the model as:

$$\dot{Q}_{RAo}\,\text{calculated} = \frac{Y\dot{Q}_{LAo} + \beta\dot{Q}_{p}}{1-Y}, \qquad (1)$$

with that obtained as the sum of directly measured flows in the main trunk of the right aorta ($\dot{Q}_{RAo,t}$) and the common carotid of one side ($\dot{Q}_{CC}$) as:

$$\dot{Q}_{RAo}\,\text{measured} = \dot{Q}_{RAo,t} + 2\dot{Q}_{CC}. \qquad (2)$$

Systemic blood flow ($\dot{Q}_s$) was taken to be the sum of measured $\dot{Q}_{RAo}$ and $\dot{Q}_{LAo}$ and was assumed to be equal to right atrial blood flow. The $\dot{Q}_s$ data thus obtained were used for analysis. Pulmonary blood flow ($\dot{Q}_p$) was calculated by doubling the flow through the left PA, on the basis of the data of Comeau and Hicks (1994), confirming that blood flow is

approximately the same between the right and left PA, irrespective of vagal stimulation. From $\dot{Q}_p$ and $\dot{Q}_s$ and the above fractional blood partitioning values, blood distribution within the ventricle was calculated in terms of absolute flow rates.

Statistics

Analysis of variance (ANOVA) with randomized block design was used to detect differences in measured and calculated parameters between experimental conditions. Dunnett and Bonferroni tests were used for pairwise comparison, as appropriate. A paired *t*-test was used to detect any significant difference between two variables obtained under the same conditions. Curve-fitting was performed using SigmaPlot for Windows (Jandel Scientific, San Rafael, CA, USA). Data are expressed as means ± S.D. wherever possible.

Results

Blood parameters in Trachemys scripta

Blood gas levels in the RAo prior to vagal sectioning are summarized in Table 1. Blood P_{O_2} and pH were in good agreement with previously determined data for the same species (Hicks and Comeau, 1994), and the acid–base status agreed well with the values interpolated from the data for chronically cannulated *Chrysemys picta bellii* (Glass *et al.* 1985). The blood P_{O_2} was found to be lower by 10 mmHg (1.3 kPa) than that of *Chrysemys picta bellii* (Glass *et al.* 1985). The fact that P_{O_2} was 50 mmHg (6.7 kPa) lower than in mechanically ventilated *P. scripta* (Hicks and Comeau, 1994) is at least partially attributable to differences in the oxygen concentration of the ventilation gas mixture (17 % O_2 in this study *versus* 21 % O_2 in Hicks and Comeau, 1994).

Pulmonary blood flow ($\dot{Q}_p$) varied, averaging 42±14 ml min^{-1} kg^{-1} (mean ± S.D., *N*=7), which is 14 ml min^{-1} kg^{-1} lower than the value reported for similarly prepared *P. scripta* by Hicks and Comeau (1994). Systemic blood flow ($\dot{Q}_s$) was 20±6 ml min^{-1} kg^{-1}. Detailed data on the haemodynamic variables of the animals are given in Hicks *et al.* (1996). Since the aim of the present study was to analyse patterns of intraventricular blood distribution under various conditions, no attempt was made to normalize the physiological conditions of the animals at the beginning of the experiment.

Table 1. *Arterial blood variables of the turtles prior to vagal sectioning*

P_{O_2}	75±3 mmHg
P_{CO_2}	25±3 mmHg
pH	7.68±0.05
$[HCO_3^-]$	35±3 mmol l^{-1}
Haematocrit	31±4 %

Values are for the right aortic blood. Mean ± S.D. (*N*=7).
1 mmHg=0.133 kPa.

Values for P_{O_2} in blood from the RAo and LAo are presented in Fig. 1. A paired *t*-test revealed that the mean P_{O_2} of the RAo (70±8 mmHg, 9.3±1.1 kPa) was significantly higher than that of the LAo (64±12 mmHg, 8.5±1.6 kPa; $P<0.001$, $N=43$). Thus, the three outflow vessel model described in Materials and methods is applicable to the present data set.

Relationship between calculated and measured $\dot{Q}_{RAo}$

The relationship between calculated and measured $\dot{Q}_{RAo}$ is presented in Fig. 2. The correlation coefficient (r) between the two variables is 0.715 ($P<0.01$). The ratio of calculated to measured values was 1.10±0.77 (mean ± S.D.).

Relationship of blood flow partitioning and cardiac output

$\dot{Q}_s$ and $\dot{Q}_p$ were similar below a $\dot{Q}_{tot}$ value of approximately 30 ml min^{-1} kg^{-1} but progressively deviated at higher values of

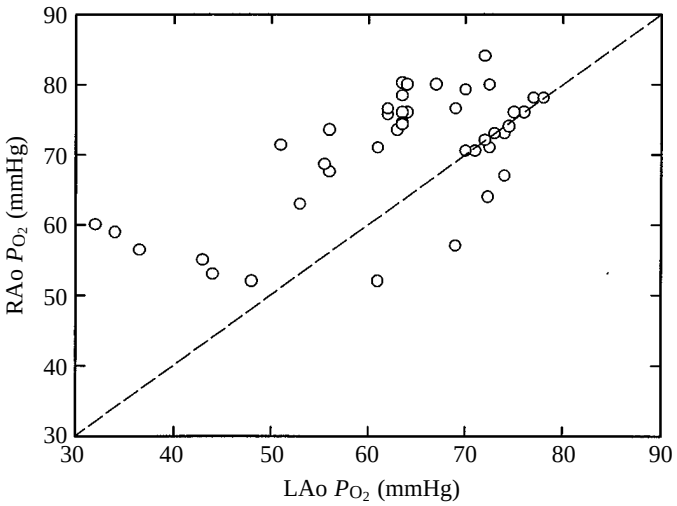

Fig. 1. Comparison of blood P_{O_2} simultaneously sampled from the right (RAo) and left (LAo) aortae. 1 mmHg=0.133 kPa.

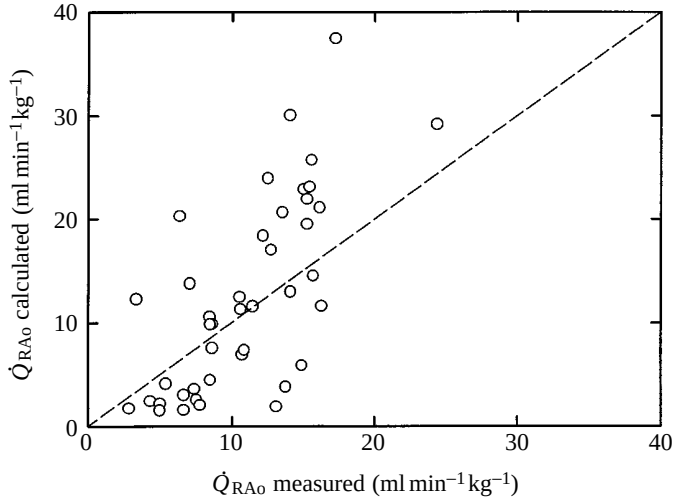

Fig. 2. Relationship between right aortic blood flow, obtained from model calculations ($\dot{Q}_{RAo}$ calculated) and by direct measurement ($\dot{Q}_{RAo}$ measured). For details, see text.

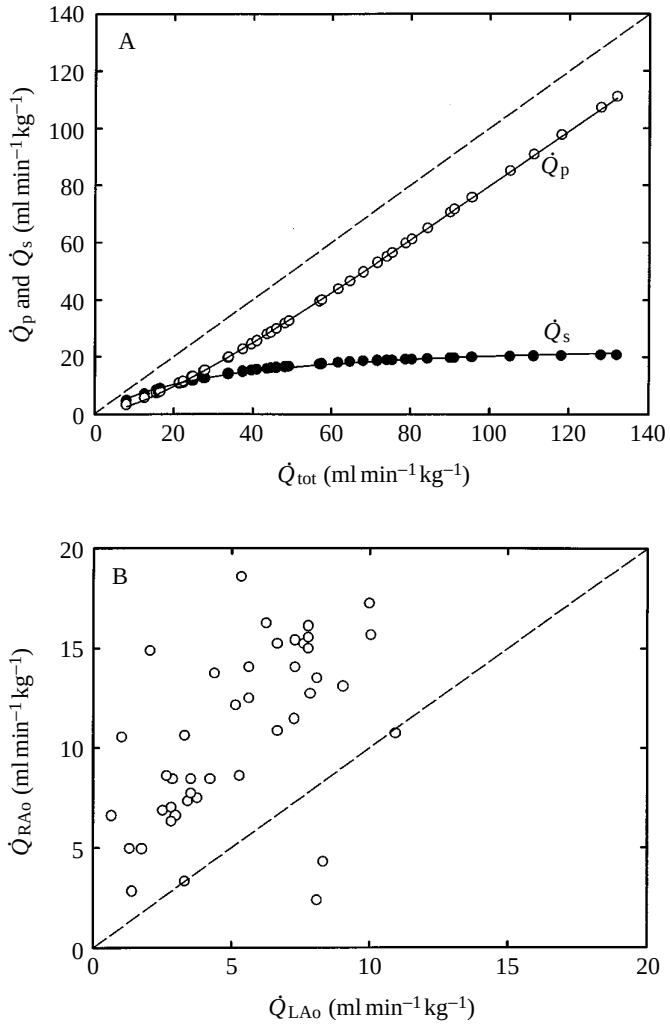

Fig. 3. (A) Pulmonary ($\dot{Q}_p$, open circles) and systemic ($\dot{Q}_s$, filled circles) blood flows as functions of total cardiac output ($\dot{Q}_{tot}$). Curves fitted by the equations in the text are also drawn. Means ± S.D. for parameters, and dependencies, for each curve are as follows: for $\dot{Q}_s$ *versus* $\dot{Q}_{tot}$, 26.49±1.73, 31.01±5.67: r=0.887. For $\dot{Q}_p$ *versus* $\dot{Q}_{tot}$, 4.52±4.07, 31.01±5.67: r=0.979 (see text). (B) Relationship between blood flow in the right aorta ($\dot{Q}_{RAo}$) and blood flow in the left aorta ($\dot{Q}_{LAo}$). Both are measured values.

$\dot{Q}_{tot}$ (Fig. 3A). The data were fitted by the following curves shown in Fig. 3A (for S.D. of the parameters and dependencies of the curves, see legend to Fig. 3A):

$$\dot{Q}_s = \frac{26.49\dot{Q}_{tot}}{31.01 + \dot{Q}_{tot}}, \quad (3)$$

$$\dot{Q}_p = \left(\frac{4.52 + \dot{Q}_{tot}}{31.01 + \dot{Q}_{tot}}\right) \times \dot{Q}_{tot}. \quad (4)$$

Since $\dot{Q}_s$ and $\dot{Q}_p$ can be expressed as functions of $\dot{Q}_{tot}$, we chose $\dot{Q}_{tot}$ as an independent variable for the following analyses. $\dot{Q}_{RAo}$ was significantly higher than $\dot{Q}_{LAo}$ (P<0.01, paired t-test, Fig. 3B).

The distribution of LAt blood into the three outflow vessels is plotted against $\dot{Q}_{tot}$ in terms of partition fractions (Fig. 4A–C) and volume flow partitioning (Fig. 4D–F). As $\dot{Q}_{tot}$ rose to approximately 40–50 ml min^{-1} kg^{-1}, the fraction α, flowing to the PA, increased sharply with increasing $\dot{Q}_{tot}$ to values as high as 0.7–0.8, but then levelled off (Fig. 4A). The fraction β, flowing to the LAo, varied considerably at low $\dot{Q}_{tot}$, ranging from below 0.1 to above 0.9, but at higher $\dot{Q}_{tot}$ the variation was greatly reduced, with values for β being close to 0.2 (Fig. 4B). A similar but less variable pattern was found for 1–α–β (Fig. 4C). Flow into the PA ($\dot{Q}_p$×α, unidirectional L–R shunt) increased linearly with $\dot{Q}_{tot}$ (Fig. 4D). Flow into the RAo ($\dot{Q}_p$×β) was similar to the flow into the LAo [$\dot{Q}_p$(1–α–β)] when $\dot{Q}_{tot}$ was lower than 40 ml min^{-1} kg^{-1}, but rose at higher $\dot{Q}_{tot}$ values (Fig. 4E,F, see figure legend for equations for regression lines).

The distribution of RAt blood into the three outflow vessels is plotted against $\dot{Q}_{tot}$ in Fig. 5. The turtles never developed a large net R–L shunt as reported in earlier *in vivo* studies (e.g. White *et al.* 1989). In only one animal was a high X+Y value of 0.55 attributable to a high X value (Fig. 5A), while in all the others X+Y was approximately 0.2. At larger values of $\dot{Q}_{tot}$, both X and Y were well below 0.1, resulting in a value of 1–X–Y approaching 1 (Fig. 5C). The PA blood flow originating from the RAt [$\dot{Q}_s$(1–X–Y)] increased sharply as $\dot{Q}_{tot}$ became larger (Fig. 5F). The blood flows into the LAo

Table 2. *Effect of vagal stimulation on partition fractions*

	X	Y	1–X–Y	α	β	1–α–β
V_{intact}	0.04±0.05	0.02±0.02	0.94±0.02	0.55±0.13	0.31±0.16	0.14±0.07
V_{cut}	0.02±0.02	0.01±0.01	0.97±0.03	0.57±0.13	0.27±0.11	0.17±0.10
RVEF	0.13±0.19	0.06±0.06	0.81±0.17	0.36±0.19	0.42±0.30	0.22±0.16
LVEF	0.04±0.03	0.01±0.01	0.95±0.04	0.55±0.18	0.19±0.09	0.26±0.15
RVAF	0.01±0.01	0.03±0.04	0.96±0.04	0.66±0.15	0.25±0.10	0.09±0.05
LVAF	0.02±0.02	0.004±0.01	0.98±0.02	0.67±0.07	0.26±0.07	0.07±0.02

Values as mean ± S.D.

V_{intact}, prior to vagal sectioning (N=6); V_{cut}, following vagal sectioning (N=7); RVEF, efferent stimulation of the right vagus (N=7); LVEF, efferent stimulation of the left vagus (N=7); RVAF, afferent stimulation of the right vagus (N=5); LVAF, afferent stimulation of the left vagus (N=7).

The partition fractions X, Y, α and β are defined in the text.

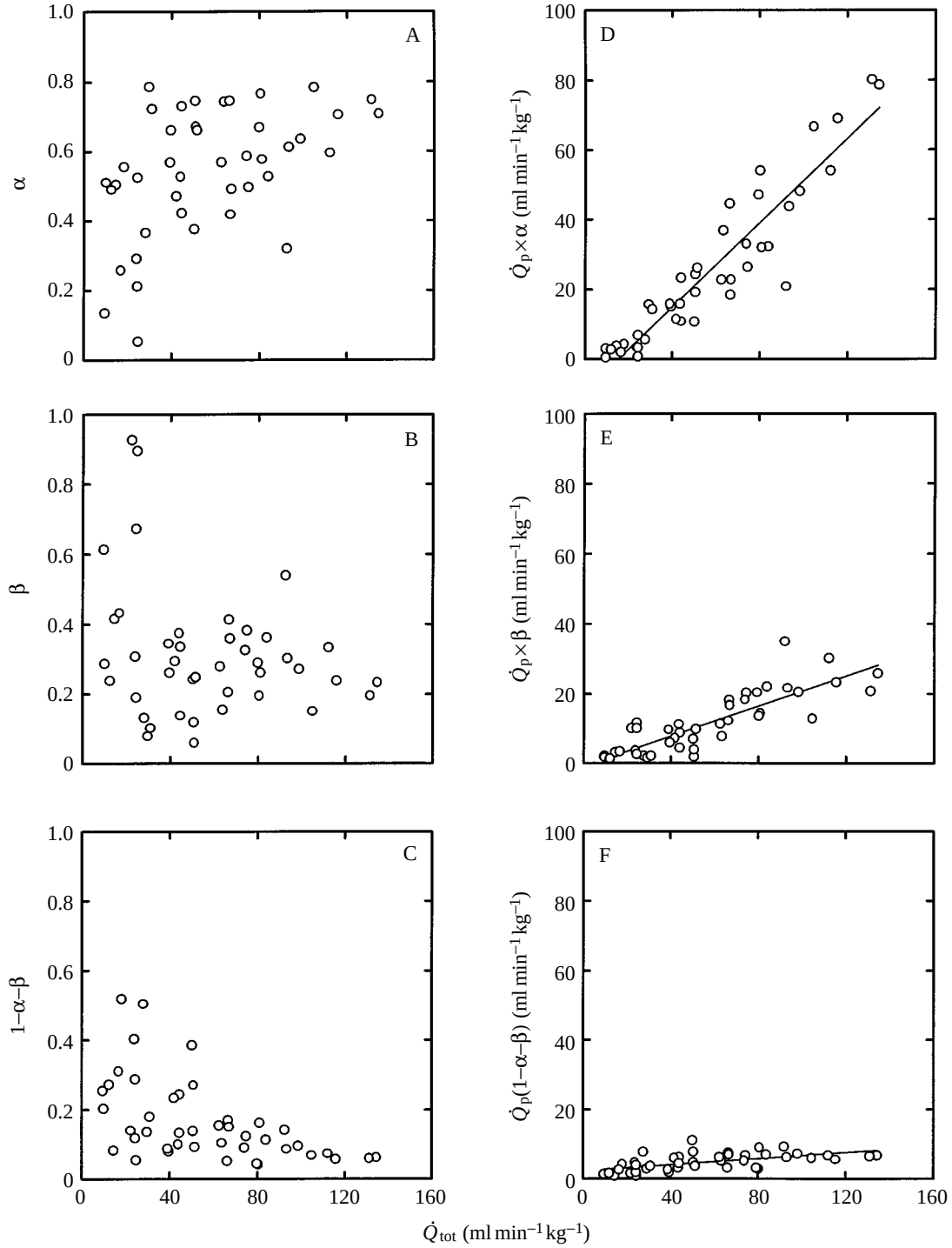

Fig. 4. Relationships between total cardiac output ($\dot{Q}_{tot}$) and fractional partition values (A, α; B, β; and C, 1–α–β) and volume partition values [D, $\dot{Q}_p\times\alpha$; E, $\dot{Q}_p\times\beta$; and F, $\dot{Q}_p(1-\alpha-\beta)$] for left atrial blood. Equations for the regression lines are as follows: D, $y=-9.34+0.605x$ ($P<0.01$); E, $y=-0.956+0.218x$ ($P<0.01$); F, $y=2.21+0.044x$ ($P<0.01$).

($\dot{Q}_s\times X$) and RAo ($\dot{Q}_s\times Y$) were low, as expected from the observed low partition fractions (Fig. 5D,E), and were not significantly dependent on $\dot{Q}_{tot}$ (see figure legend).

Effect of vagal stimulation on partition fraction values (Table 2)

Of the six partition fraction values, 1–*X*–*Y* showed the largest change in response to vagal stimulation. The mean 1–*X*–*Y* value (0.81) during RVEF was significantly lower than the values measured under all the other conditions ($P<0.05$, Bonferroni test in a randomized block design ANOVA). The value of 1–*X*–*Y* was highly constant during the other periods and there were no significant differences between any pair of values ($P>0.05$). *X* and β were not significantly affected by vagal stimulation ($P>0.05$). The very large variability of *X*, particularly for RVEF, is due to an exceptionally high value from one animal. If this value is disregarded, the mean partition fraction value *X* during RVEF was 0.062±0.042. This is not significantly different from the values found during the other periods. Values of *Y* were significantly different only between

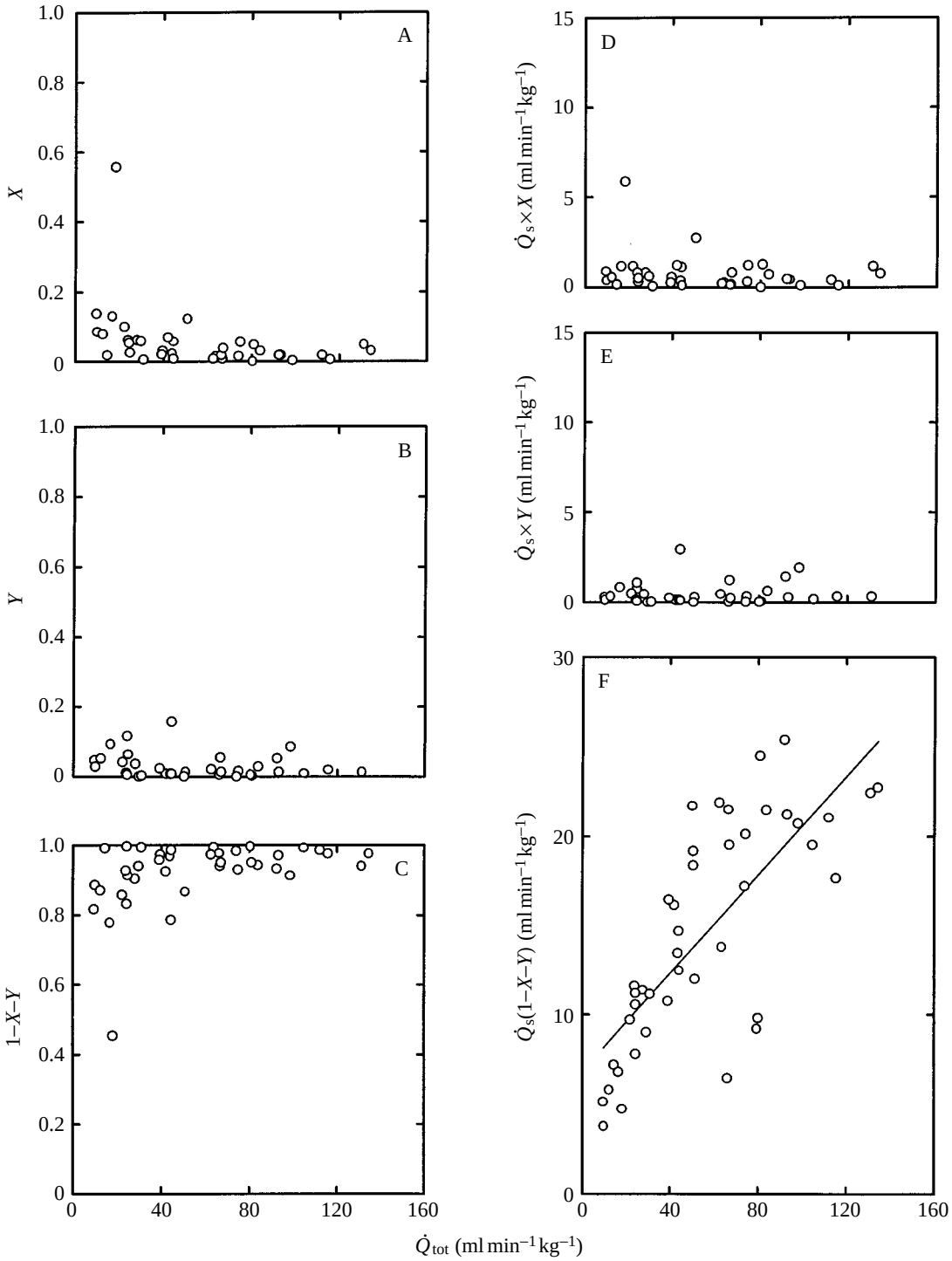

Fig. 5. Relationships between total cardiac output ($\dot{Q}_{tot}$) and fractional partition values (A, *X*; B, *Y*; and C, 1–*X*–*Y*) and volume partition values [D, $\dot{Q}_s \times X$; E, $\dot{Q}_s \times Y$; and F, $\dot{Q}_s(1–X–Y)$] for right atrial blood. The equation for the regression line in F is: $y=6.84+0.137x$ ($P<0.01$). The slopes of regression lines for D and E are not significant: D, $P=0.24$; E, $P=0.852$.

RVEF and LVAF ($P<0.05$). Values of α were significantly different between RVEF and LVAF ($P<0.01$), as well as between RVEF and RVAF ($P<0.05$). Significant differences in 1–α–β were found in all three pairwise comparisons, between RVEF and LVAF ($P<0.05$), between RVAF and LVEF ($P<0.01$), and between LVEF and LVAF ($P<0.01$).

Blood oxygen levels as a function of cardiac output

P_{O_2} in the LAt was statistically independent of $\dot{Q}_{tot}$ at approximately 80 mmHg (10.7 kPa; Fig. 6D), while P_{O_2} in the RAt changed significantly as a function of $\dot{Q}_{tot}$ (Fig. 6D, see figure legend for regression equation). Only at low $\dot{Q}_{tot}$, where the partition fraction value *Y* indicated some increase (see Fig. 5B), did P_{O_2} in the RAo differ from P_{O_2} in the LAt (Fig. 6A). P_{O_2} in the LAo was lower than that in the LAt at low $\dot{Q}_{tot}$ (Fig. 6B). The difference in P_{O_2} between PA and LAt remained at approximately 30 mmHg (4 kPa) at $\dot{Q}_{tot}$ values of more than approximately 40 ml min^{-1} kg^{-1}, but at lower $\dot{Q}_{tot}$ there was a tendency for this difference to increase (Fig. 6C).

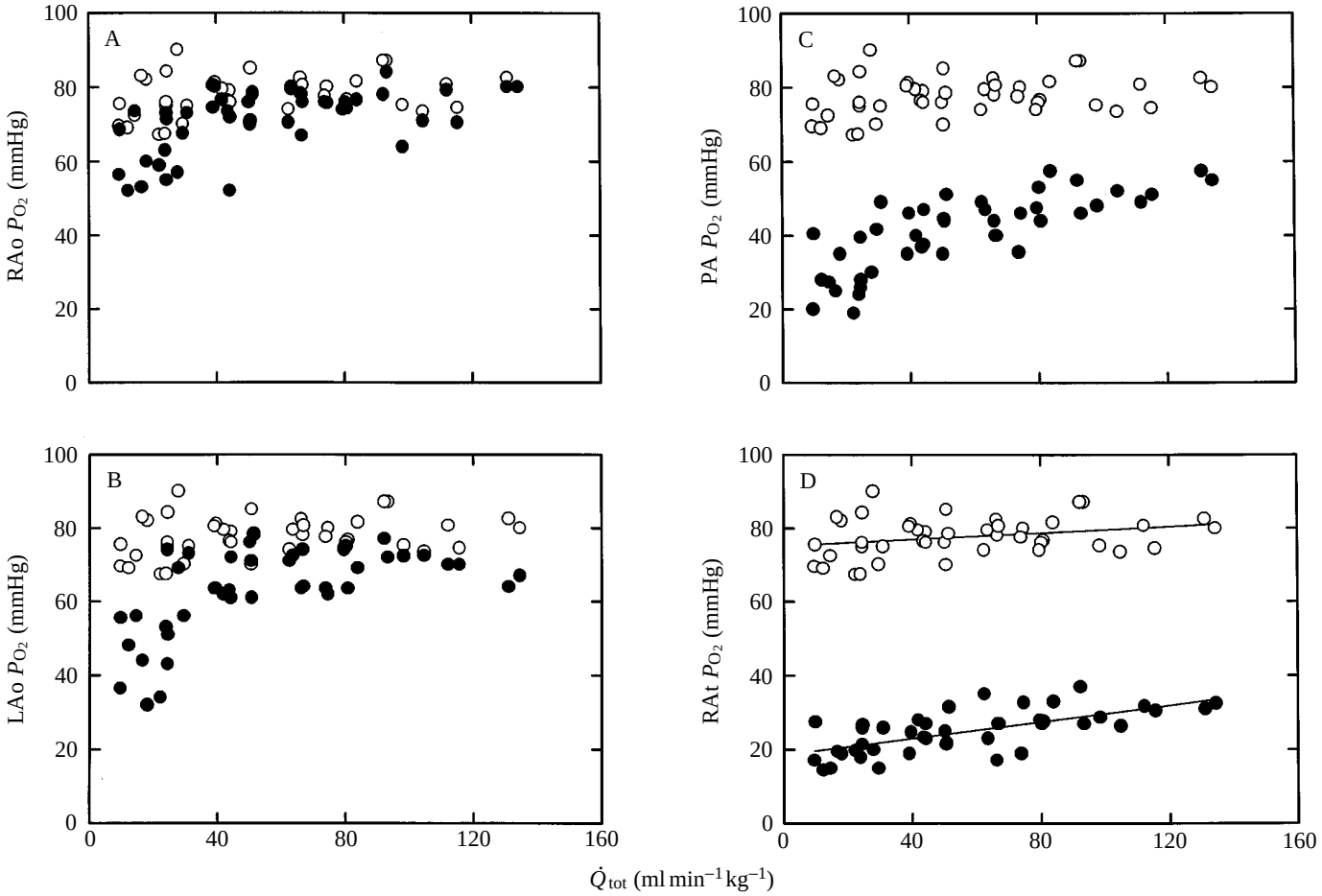

Fig. 6. Relationships between total cardiac output ($\dot{Q}_{tot}$) and blood P_{O_2} of (A) the right aorta (RAo), (B) the left aorta (LAo), (C) the pulmonary artery (PA) and (D) the right atrium (RAt). Open circles represent left atrial (LAt) P_{O_2} in all the graphs. The equation for the regression line for RAt *versus* $\dot{Q}_{tot}$ is: y=18.7+0.11x (P<0.01). 1 mmHg=0.133 kPa.

Effect of vagal stimulation on blood P_{O_2} *(Fig. 7)*

P_{O_2} in the LAt was not affected by vagal stimulation and, accordingly, values are not presented (P>0.05, Bonferroni test in a randomized block design ANOVA). In only two cases could differences that were statistically significant be detected in values for RAt P_{O_2} determined during different stimulation periods: V_{intact} *versus* LVEF and RVEF (P<0.05) (not shown in Fig. 7). Differences in LAo P_{O_2} between RVEF and all other treatments were highly significant (P<0.01). As a result, the difference in P_{O_2} between the LAt and LAo blood became significantly larger during RVEF compared with the values found in the other conditions (P<0.01). P_{O_2} in the RAo was lowered by RVEF, but the resulting differences were only significant between V_{intact} and RVEF, between V_{cut} and RVEF and between LVAF and RVEF (P<0.05). The differences in PA P_{O_2} measured during RVEF and under all other conditions were significant (P<0.05), except between LVEF and RVEF.

LAt P_{O_2} was unaffected by vagal stimulation (overall mean 78±5 mmHg (10.4±0.7 kPa, N=40). RAt was also stable except for a small decline in response to LVEF and RVEF. Overall mean values for RAt P_{O_2} were 28±5 mmHg (3.7±0.7 kPa, N=25) for all conditions except LVEF and RVEF and 22±5 mmHg (2.9±0.7 kPa, N=14) for these two conditions.

The oxygen content, calculated for blood from the LAt (LAt C_{O_2}), was not significantly different during RVEF from that during any other condition (P>0.05). The oxygen content of RAt blood (RAt C_{O_2}) during V_{intact} differed significantly from values during RVEF (P<0.05) and RVAF (P<0.01).

Discussion

Accuracy of model calculations

In several cases, large discrepancies were found between calculated and measured $\dot{Q}_{RAo}$ (Fig. 2). Checking these instances against data sets with better agreement revealed no apparent relationship with the absolute values of variables, except for indicating a correlation coefficient (r) of 0.61 for $\dot{Q}_p$ (P<0.01). Indirect estimation of oxygen content is subject to errors in the determination of P_{O_2} and pH in addition to errors introduced by data from the oxygen dissociation curve. The effect of such errors on the estimation of partition fractions becomes larger at high $\dot{Q}_p$ because the differences in C_{O_2}

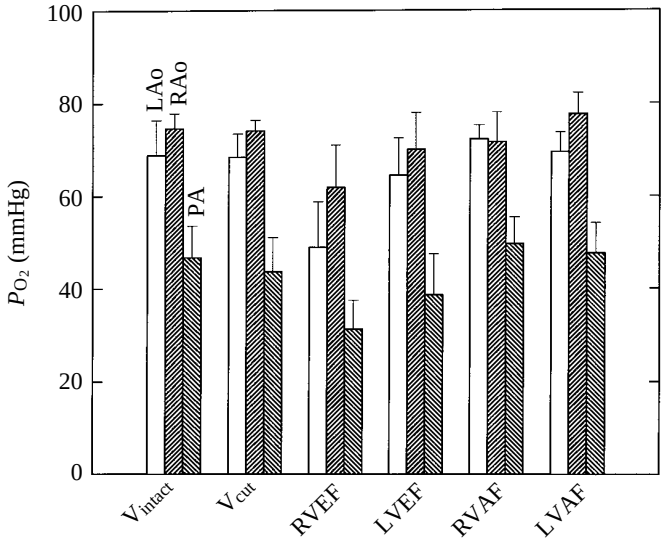

Fig. 7. Effects of vagal stimulation on P_{O_2} in the right aorta (RAo), the left aorta (LAo) and the pulmonary artery (PA). Values are means + S.D. 1 mmHg=0.133 kPa.

between two sites become smaller under these conditions (Fig. 6), introducing larger deviations in the equations for partition fractions in addition to $\dot{Q}_{PA}/\dot{Q}_{LAo}$ (the partition fraction representing a R–L shunt, see Ishimatsu *et al.* 1988).

However, the differences found may also be related to slight violations of the boundary conditions of the model. There are two fundamental conditions for the validity of the vessel model: (1) conservation of mass (blood volume and amount of oxygen) during blood transit through the ventricle and (2) no net fluid movement through the peripheral capillary walls. If a significant fraction of the pulmonary circulation were filtered through the capillary walls, as claimed for the lungs of *Trachemys scripta* (Burggren, 1982), some degree of deviation would be expected.

Relationship between cardiac shunting and blood gas levels in the three outflow vessel model

The difference in P_{O_2} between LAt and LAo blood during RVEF was very significantly larger than under any other condition. The data on the partition fractions suggest that this was not caused by changes in partitioning pertaining to the LAo (X and $1-\alpha-\beta$, see Table 2). The oxygen content of mixed blood ejected into an outflow vessel is a function of the oxygen content and relative volume of the two inputs. The relative volume, in turn, is determined not only by the partition fractions of that vessel but also by the contributions of systemic and pulmonary flow to the flow rate in the vessel. Thus, oxygen content of LAo blood (LAo C_{O_2}) is:

$$\text{LAo } C_{O_2} = \frac{\dot{Q}_s}{\dot{Q}_{LAo}} \times X \times \text{RAt } C_{O_2} + \frac{\dot{Q}_p}{\dot{Q}_{LAo}} \times (1-\alpha-\beta) \times \text{LAt } C_{O_2}. \quad (5)$$

Vagal stimulation did not affect calculated values of LAt C_{O_2}, and values for RAt C_{O_2} measured during RVEF differed only from the value measured during V_{intact}. Consequently, the major, if not exclusive, factor contributing to a significant fall in LAo P_{O_2} (and C_{O_2}) during RVEF is the ratio $\dot{Q}_s/\dot{Q}_p$.

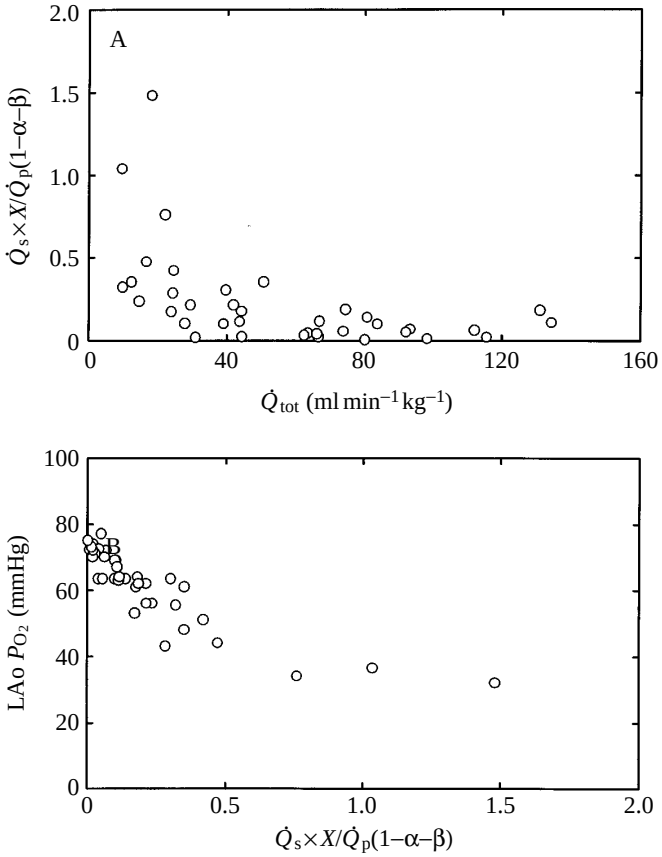

Fig. 8. (A) Relationship between total cardiac output ($\dot{Q}_{tot}$) and the ratio $\dot{Q}_s \times X/\dot{Q}_p(1-\alpha-\beta)$. Note the sharp increase in the ratio below a $\dot{Q}_{tot}$ of 40 ml min^{-1} kg^{-1}. (B) Relationship between the ratio $\dot{Q}_s \times X/\dot{Q}_p(1-\alpha-\beta)$ and left aorta (LAo) P_{O_2}. 1 mmHg=0.133 kPa.

Since LAt C_{O_2} generally exceeds RAt C_{O_2}, LAo C_{O_2} should be lower, as the ratio of $\dot{Q}_s \times X$ to $\dot{Q}_p(1-\alpha-\beta)$ increases, and *vice versa*. There was a clear tendency for the ratio to increase when $\dot{Q}_{tot}$ fell below approximately 40 ml min^{-1} kg^{-1} (Fig. 8A). An inverse relationship between P_{O_2} in the LAo and this ratio is clearly demonstrated in Fig. 8B. Similar relationships exist for the other two outflow vessels (RAo and PA, data not shown).

The idea that changing the ratio $\dot{Q}_s/\dot{Q}_p$ has an effect on the oxygen content of the outflowing blood in the three outflow vessel model is important. Changes in the levels of blood oxygen in the cardiac outflow vessels of reptiles and other animals with cardiac shunts are usually explained by changes in partition fractions. For instance, the lowering of systemic blood oxygen levels has usually been interpreted as resulting from increasing partition fractions for the R–L shunt (e.g. White *et al.* 1989). However, this is true only when the two aortic arches have the same blood oxygen level. Only then is the partition fraction representing a R–L shunt (R) the sole

determinant of systemic oxygen levels, given that the oxygen content of the LAt and RAt blood are constant. The oxygen content of the systemic arterial blood (SA C_{O_2}) is determined by:

$$\text{SA } C_{O_2} = R \times \text{RAt } C_{O_2} + (1-R)\text{LAt } C_{O_2}. \quad (6)$$

A similar relationship is valid for the oxygen content of the pulmonary arterial blood (PA C_{O_2}):

$$\text{PA } C_{O_2} = (1-L)\text{RAt } C_{O_2} + L \times C_{\text{LAt}}, \quad (7)$$

where L is the partition fraction for the flow from LAt to PA. However, evidence exists for Reptilia (Ishimatsu *et al.* 1988, as well as earlier papers cited in the Introduction) and Amphibia (DeLong, 1962; Haberich, 1965; W. W. Burggren, personal communication) that blood from the RAt and LAt is differentially partitioned towards the two systemic arches. If so, the above two formulae are not applicable. For example, a lowering of the P_{O_2} in the LAo (but not the RAo) was reported in response to vagal stimulation eliciting propagation of ventricular depolarization associated with apnoea (Burggren, 1978). For this situation, the three outflow vessel model predicts that the reported lowering of LAo P_{O_2} could have resulted from an increase in X, a decrease in $1-\alpha-\beta$, an increase in the ratio $\dot{Q}_s/\dot{Q}_p$ or a combination of these possibilities.

Significance of the present findings

To our knowledge, this is the first complete description of blood flow partitioning within the turtle ventricle. The extensively invasive nature of the present technique makes it difficult to apply the method to recovered animals, but the information obtained from the present study forms the basis for a detailed analysis of the mechanisms involved in cardiac shunting in turtles.

The present analysis clarifies the complex relationship between the partitioning of blood from the two atrial inflow tracts towards the three cardiac output pathways. In the turtle, in most instances, blood shunting occurs simultaneously in both directions (R–L and L–R shunts) as previously found in *Varanus niloticus* (Ishimatsu *et al.* 1988). Where $\dot{Q}_{tot}$ is lower than 30 ml min^{-1} kg^{-1}, α varies from below 0.1 to almost 0.6, and X and Y showed some positive values (Figs 4, 5) at which $\dot{Q}_p$ and $\dot{Q}_s$ were approximately the same (cf. Fig. 2). Patterns of blood mixing should therefore be carefully discriminated from net volume shunts. Net volume shunt relates to differences between $\dot{Q}_p$ and $\dot{Q}_s$, and may be zero when there is substantial blood mixing in both directions.

Simultaneous measurement of $\dot{Q}_p$ and $\dot{Q}_s$ can provide information on net shunting, but will not detect unidirectional blood mixing. Conversely, oxygen analysis of the blood in the central vascular site can, on its own, provide partition fractions only when blood gas levels are identical in the two systemic arches. In other cases, additional information is required; for example, that obtained by application of the microsphere method to assess partition fraction values. Even then, an estimate of absolute volume flow cannot be made. Accordingly, a combination of blood gas analysis and flow measurement is required to obtain a full, quantitative picture of cardiac shunting as presented in this study.

With increasing $\dot{Q}_{tot}$, $1-X-Y$ approached 1.0 while α reached a maximum value of approximately 0.8. Under these conditions, all RAt blood would be ejected into the PA whereas 20 % of the LAt blood would be directed into the systemic arches. Although theoretically possible, a total shutdown of systemic circulation and exclusive perfusion of the pulmonary circuit did not actually take place. In contrast, there is apparently an upper limit for $\dot{Q}_s$, above which $\dot{Q}_p$ increases $\dot{Q}_{tot}$ linearly within the blood flow range covered by this study. The differences in blood oxygen levels (Fig. 1) and flow rates (Fig. 3B) between the two systemic arches enables a preferential supply of oxygen to the upper body mass, including the central nervous system.

With increasing $\dot{Q}_{tot}$, the P_{O_2} in PA blood rises above RAt P_{O_2}, indicating recirculation of pulmonary venous blood back into the pulmonary circuit (Fig. 6). Hicks *et al.* (1996) have demonstrated that a net L–R shunt is a function of $\dot{Q}_{tot}$. Fig. 9 plots the X, Y and α values against percentage volume flow in the pulmonary blood circuit ejected before the systemic blood flow starts ($\%\dot{Q}_{ppre}$). Nine data points, determined simultaneously in the same individual, were available. α apparently increased with $\%\dot{Q}_{ppre}$ (Fig. 9C), while Y decreased with $\%\dot{Q}_{ppre}$ (Fig. 9B). There was no apparent relationship between X and $\%\dot{Q}_{ppre}$ (Fig. 9A). Regression analysis revealed a significant linear relationship between $\dot{Q}_{tot}$ and $\%\dot{Q}_{ppre}$ ($\%\dot{Q}_{ppre}=-4.51+0.128\dot{Q}_{tot}$, $P<0.05$; not shown). It should be noted that the flow from the LAt to the PA ($\dot{Q}_p \times \alpha$) far exceeded the flows from the RAt to the RAo or the LAo ($\dot{Q}_s \times X$ or $\dot{Q}_s \times Y$) when $\dot{Q}_{tot}$ was greater than 30–40 ml min^{-1} kg^{-1} (Figs 3A, 5). Thus, at high $\dot{Q}_{tot}$, relatively small volumes of RAt blood residing in the CV at the end of diastole would be conveyed into the CP or even into the pulmonary circuit by movement of blood within the ventricle induced by the earlier ejection into the PA. This blood movement (counter-clockwise, viewed from the atrium) and the position of the RAo opening (lying further 'upstream' than that of the LAo) may be partly responsible for the higher oxygen levels in this arch. It has been pointed out that blood ejection into the pulmonary circuit precedes that into the systemic circuit by about 50–150 ms in Reptilia (Johansen *et al.* 1970; Shelton and Burggren, 1976; Ishimatsu *et al.* 1988; Hicks *et al.* 1996).

Angiographic observations (Hicks *et al.* 1996) have demonstrated that opaque material, injected into the CA just before pulmonary ejection during stimulation of vagal afferent nerves, flowed as a thin streak into the PA. This clearly indicates translocation of the material from the CA into the CP. During early systole, the muscular ridge evidently did not abut the opposing ventricular wall. At the end of systole, the CD is totally filled by LAt blood. During the next diastole, LAt blood lying in the CV will be washed into the CP (the washout mechanism, Heisler *et al.* 1983; Heisler and Glass, 1985). The extent of blood movement would be affected by (1) the ejection

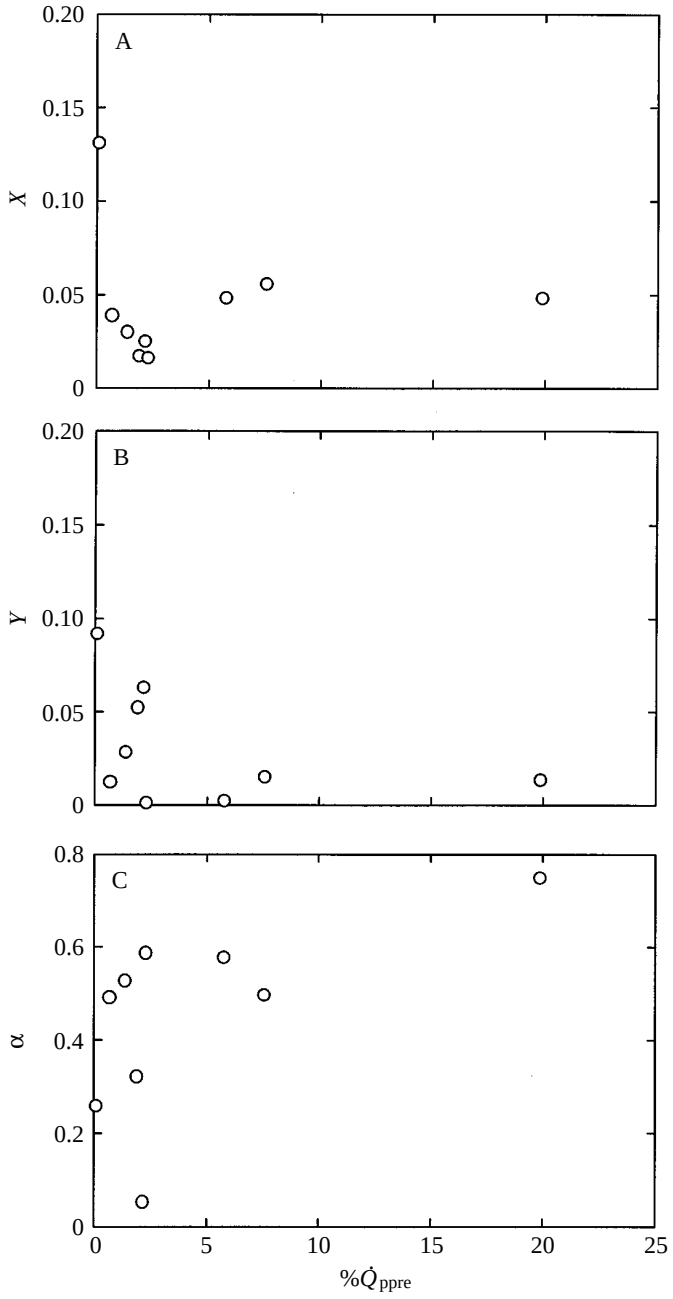

Fig. 9. Relationships between *X*, *Y* and α and percentage blood flow in the pulmonary circuit ejected before systemic blood flow starts (%$\dot{Q}_{ppre}$). The data were obtained from three turtles in which these two parameters were determined simultaneously.

timing differences which, in turn, are influenced by the difference in diastolic pressures between the pulmonary and systemic circuits (Hicks *et al.* 1996), (2) the vascular resistance of the pulmonary circuit, (3) the contractility of the ventricular myocardium, and possibly (4) the direction of propagation of the excitation wave, as found by Burggren (1978).

In vivo studies have shown that, under certain conditions (e.g. during ventilation), $\dot{Q}_p$ greatly exceeds $\dot{Q}_s$ (Shelton and Burggren, 1976; West *et al.* 1992). Such physiological states may result in a blood distribution pattern similar to that seen in mammals and birds, where the systemic circuit is perfused exclusively with LAt blood and the whole volume of RAt blood is directed into the pulmonary circulation. A perfusion pattern such as this, which would be advantageous for gas exchange, would entail L–R shunting in turtles, as depicted by the present study.

Note added in proof

$\dot{Q}_s/\dot{Q}_p$ can be expressed using only partition fractions as $(1-\alpha)/(1-X-Y)$. Thus,

$$\frac{\dot{Q}_s \times X}{\dot{Q}_p(1-\alpha-\beta)} = \frac{1-\alpha}{1-X-Y} \times \frac{X}{1-\alpha-\beta}. \quad (8)$$

This means that blood oxygen levels in the LAo are affected not only by the ratio of partition fractions for the vessel $[X/(1-\alpha-\beta)]$, but also by the ratio of unshunted fractions $[(1-\alpha)/(1-X-Y)]$.

We would like to thank Professor J. Piiper for invaluable discussion. This research was supported by Deutsche Forschungsgemeinschaft.

References

BAKER, L. A. AND WHITE, F. N. (1970). Redistribution of cardiac output in response to heating in *Iguana iguana*. *Comp. Biochem. Physiol.* **35**, 253–262.

BURGGREN, W. W. (1978). Influence of intermittent breathing on ventricular depolarization patterns in chelonian reptiles. *J. Physiol., Lond.* **278**, 349–364.

BURGGREN, W. W. (1982). Pulmonary blood plasma filtration in reptiles: A 'wet' vertebrate lung? *Science* **215**, 77–78.

BURGGREN, W., HAHN, C. E. W. AND FOËX, P. (1977). Properties of blood oxygen transport in the turtle *Pseudemys scripta* and the tortoise *Testudo graeca*: Effects of temperature, CO_2 and pH. *Respir. Physiol.* **31**, 39–50.

BURGGREN, W. W. AND SHELTON, G. (1979). Gas exchange and transport during intermittent breathing in chelonian reptiles. *J. exp. Biol.* **82**, 75–92.

COMEAU, S. G. AND HICKS, J. W. (1994). Regulation of central vascular blood flow in the turtle. *Am. J. Physiol.* **267**, R569–R578.

DELONG, K. T. (1962). Quantitative analysis of blood circulation through the frog heart. *Science* **138**, 693–694.

GLASS, M. L., BOUTILIER, R. G. AND HEISLER, N. (1985). Effects of body temperature on respiration, blood gases and acid–base status in the turtle *Chrysemys picta bellii*. *J. exp. Biol.* **114**, 37–51.

HABERICH, F. J. (1965). The functional separation of venous and arterial blood in the univentricular frog heart. *Ann. N. Y. Acad. Sci.* **127**, 459–476.

HEISLER, N. AND GLASS, M. L. (1985). Mechanism and regulation of central vascular shunts in reptiles. In *Cardiovascular Shunts: Phylogenetic, Ontogenetic and Clinical Aspects* (ed. K. Johansen and W. Burggren), pp. 334–353. Copenhagen: Munksgaard.

HEISLER, N., NEUMANN, P. AND MALOIY, G. M. O. (1983). The mechanism of intracardiac shunting in the lizard *Varanus exanthematicus*. *J. exp. Biol.* **105**, 15–31.

HICKS, J. W. AND COMEAU, S. G. (1994). Vagal regulation of

intracardiac shunting in the turtle *Pseudemys scripta*. *J. exp. Biol.* **186**, 109–126.

HICKS, J. W., ISHIMATSU, A., MOLLOI, S., ERSKIN, A. AND HEISLER, N. (1996). The mechanism of cardiac shunting in reptiles: a new synthesis. *J. exp. Biol.* **199**, 1435–1446.

HICKS, J. W. AND MALVIN, G. M. (1992). Mechanism of intracardiac shunting in the turtle *Pseudemys scripta*. *Am. J. Physiol.* **262**, R986–R992.

ISHIMATSU, A., HICKS, J. W. AND HEISLER, N. (1988). Analysis of intracardiac shunting in the lizard, *Varanus niloticus*: A new model based on blood oxygen levels and microsphere distribution. *Respir. Physiol.* **71**, 83–100.

JOHANSEN, K., LENFANT, C. AND HANSON, D. (1970). Phylogenetic development of pulmonary circulation. *Fedn Proc. Fedn Am. Socs exp. Biol.* **29**, 1135–1140.

KHALIL, F. AND ZAKI, K. (1964). Distribution of blood in the ventricle and aortic arches in Reptilia. *Z. vergl. Physiol.* **48**, 663–689.

MAGINNISS, L. A., SONG, Y. K. AND REEVES, R. B. (1980). Oxygen equilibria of ectotherm blood containing multiple hemoglobins. *Respir. Physiol.* **42**, 329–343.

NICOL, S. C., GLASS, M. L. AND HEISLER, N. (1983). Comparison of directly determined and calculated plasma bicarbonate concentration in the turtle *Chrysemys picta bellii* at different temperatures. *J. exp. Biol.* **107**, 521–525.

SHELTON, G. AND BURGGREN, W. W. (1976). Cardiovascular dynamics of the Chelonia during apnoea and lung ventilation. *J. exp. Biol.* **64**, 323–343.

TUCKER, V. A. (1966). Oxygen transport by the circulatory system of the green iguana (*Iguana iguana*) at different body temperatures. *J. exp. Biol.* **44**, 77–92.

VAN MIEROP, L. H. S. AND KUTSCHE, L. M. (1985). Some aspects of comparative anatomy of the heart. In *Cardiovascular Shunts: Phylogenetic, Ontogenetic and Clinical Aspects* (ed. K. Johansen and W. Burggren), pp. 38–56. Copenhagen: Munksgaard.

WEST, N. H., BUTLER, P. J. AND BEVAN, R. M. (1992). Pulmonary blood flow at rest and during swimming in the green turtle, *Chelonia mydas*. *Physiol. Zool.* **65**, 287–310.

WHITE, F. N., HICKS, J. W. AND ISHIMATSU, A. (1989). Relationship between respiratory state and intracardiac shunts in turtles. *Am. J. Physiol.* **256**, R240–R247.